Electrochemical Method for Studying the Kinetics of Electron Recombination and Transfer Reactions in Heterogeneous Photocatalysis: The Effect of Fluorination on TiO 2 Nanoporous La...

ARTICLE *in* THE JOURNAL OF PHYSICAL CHEMISTRY C · OCTOBER 2007

Impact Factor: 4.77

2 AUTHORS:

Damián Monllor-Satoca
Institut Químic de Sarrià
47 PUBLICATIONS **665** CITATIONS
SEE PROFILE

Roberto Gomez
University of Granada
94 PUBLICATIONS **3,045** CITATIONS
SEE PROFILE

Electrochemical Method for Studying the Kinetics of Electron Recombination and Transfer Reactions in Heterogeneous Photocatalysis: The Effect of Fluorination on TiO_2 Nanoporous Layers

Damián Monllor-Satoca and Roberto Gómez*

Institut Universitari d'Electroquímica i Departament de Química Física, Universitat d'Alacant, Apartat 99, E-03080 Alacant, Spain

Received: July 19, 2007; In Final Form: October 16, 2007

An electrochemical method for evaluating the rate constants of recombination and transfer to solution for electrons generated upon illumination of TiO_2 photocatalysts is presented. It is based on the combination of voltammetric measurements in the dark and open circuit photopotential relaxation measurements done with nanoporous thin film electrodes. Not only the average first-order rate constants for electron consumption are obtained in such a way but also the values of such constants as a function of the electrode potential (microcanonical rate constants). This method is applied to different titanium dioxide samples as to elucidate the effect of fluorination on the rate of both electron recombination (with surface trapped holes) and electron transfer to dissolved oxygen. In both cases, but especially for recombination, there is, upon fluorination, a significant retardation of the electron consumption process in agreement with several photocatalytic studies found in the literature. Finally, we take advantage of the obtainment of microcanonical constants to fit the theoretical Gerischer expression for the rate constant in the case of oxygen reduction on TiO_2 fluorinated surfaces.

Introduction

The photoelectrochemical behavior of nanoporous TiO_2 electrodes has been receiving increased attention since the early 90s. This is partly due to the discovery of an efficient photoelectrochemical cell for the conversion of light into electricity based on an anatase nanoporous photoanode (dye-sensitized solar cell, DSSC).[1] In addition to their interest for their application in such a device, a lot of attention has been paid to nanocrystalline oxide electrodes in connection with their potential use for water splitting[2] and for decontaminative photoelectrocatalysis.[3]

In all cases, charge carrier recombination, which is thought to occur easily at the nanoparticle surface, needs to be minimized, especially if we take into account that the nanoporous thin films are thought to present a very high volumic density of surface and grain boundary (GB) traps that may behave as recombination centers.[4−6] Moreover, in the case of heterogeneous photocatalysis, it is important to estimate the rate of interfacial electron transfer toward solution species, as this is, in most cases, the rate determining step because holes are transferred significantly faster to the electrolyte.[4] In fact, the accumulation of electrons in the nanoparticles and aggregates is reflected in a shift toward more negative values of the open circuit potential upon illumination.[7] Obviously, within this application, our main interest is to maximize the rate of electron transfer to solution acceptors (i.e., oxygen).

On the other hand, the kinetics of electron transfer and recombination reactions in DSSCs has recently been followed by two related experimental techniques: the open-circuit photovoltage decay (OCVD)[8,9] and the charge extraction method.[10] Whereas the first technique is sensitive to the concentration of free electrons, the latter can be used to determine the rate at which the total (mainly trapped) electron density decays.

The use of photopotential experiments for the investigation of photo(electro)catalysis in aqueous solutions has been rather limited and done at a qualitative or semiquantitative level.[7,11−17] On the other hand, electron accumulation in nanoporous TiO_2 films has been studied among other techniques by means of cyclic voltammetry.[18−23]

In this contribution we combine both open circuit photopotential measurements with cyclic voltammetry in the electron accumulation region as a means to obtain the decay rate for electrons in TiO_2 nanocrystalline thin films. Integration of the voltammogram allows us to determine the total electron concentration in the nanoporous film as a function of the electrode potential. We can then translate the open-circuit potential (OCP) into electron concentration in the film and obtain directly photogenerated electron concentration vs time curves.

We have applied this procedure to the case of electron recombination at different TiO_2 samples both in the presence and in the absence of fluoride. It is worth noting that fluorination has been proposed recently by several groups as a method to improve the photocatalytic activity of titanium dioxide.[24,25−37] Significant changes in the photocatalytic behavior of TiO_2 have been evidenced in most cases. Many explanations have been invoked to account for such experimental observations. The adsorption of fluoride on the TiO_2 surface has been supposed to avoid the generation of surface bound hydroxyls and to enhance the formation of solution hydroxyl radicals.[26,30,32,35] In addition, it has been mentioned that fluoride adsorption would trigger an important reduction of the positive surface charge of TiO_2 in contact with acidic solutions[30] as well as would hinder

* Corresponding author. E-mail: Roberto.Gomez@ua.es. Fax: +34 965903537.

10.1021/jp075672r CCC: $40.75
Published on Web 12/13/2007

the adsorption/complexation of the organic substrates to be photooxidized.[30,35] Finally, TiO_2 fluorination has been proposed to lead to the formation of $\equiv$Ti−F electron trapping sites, which would cause a reduction in the rates of the interfacial electron transfer, including that of recombination with intermediates or with H_2O_2.[30,33,35] The work reported here allows one to confirm, even quantitatively, some of the proposed hypotheses.

Theory

Upon illumination, the open circuit potential of a nanocrystalline TiO_2 electrode in contact with an aqueous solution shifts toward more negative values because of the preferential hole surface trapping and/or hole transfer to solution and the accumulation of electrons in the nanoparticles. The absolute value of the illumination-triggered OCP change is called in the foregoing photopotential. In a nanocrystalline electrode, the measured OCP change corresponds to a shift in the Fermi level of the nanoporous film substrate (F:SnO_2 conducting glass in our case). Therefore, only the electrons in the nanoporous film that can communicate with the substrate will contribute to the observed signal. Such electrons are expected to be those located in extended states, i.e., conduction band (CB) free electrons.[8] Then, in an ideal case, we can write the photopotential as

$$V_{ph} = E_{oc}^{dark} - E_{oc} = \frac{kT}{e} \ln \frac{n_c}{n_{c,dark}} \quad (1)$$

where n_c and $n_{c,dark}$ are the conduction band electron concentrations upon illumination and in the dark. The value of $n_{c,dark}$ will be given by

$$n_{c,dark} = N_c e^{(E_c - E_{oc}^{dark})e/kT} \quad (2)$$

where N_c is the effective density of conduction band states, E_c is the potential corresponding to the conduction band edge energy, and E_{oc}^{dark} is the open circuit potential (rest potential) of the nanocrystalline electrode. The latter will be a redox equilibrium potential in the presence of a reversible redox couple, but in general, it will be a mixed potential resulting from all the half-reactions taking place at the nanoparticles. As observed, we are assuming that a Maxwell−Boltzmann distribution applies. Therefore, we are considering that TiO_2 behaves as a nondegenerate semiconductor even when electrons are accumulating in the conduction band under illumination at open circuit. The electron concentrations attained in our case (lower than 10^{19} cm^{-3}) are well below the concentrations needed for degeneracy, especially on account of the large effective mass of TiO_2 conduction band electrons.

We may write down eq 1 in terms of the concentration of CB photogenerated electrons ($n_{c,ph} = n_c - n_{c,dark}$), resulting in

$$V_{ph} = \frac{kT}{e} \ln\left(1 + \frac{n_{c,ph}}{n_{c,dark}}\right) \quad (3)$$

The kinetics of electron recombination or transfer to solution could, in principle, be extracted from V_{ph} vs t relaxation curves recorded upon light interruption. In fact, the concentration of electrons is expected to drop due to recombination with photogenerated trapped holes (h_s^+) (or species resulting from them, such as adsorbed peroxo and adsorbed or solution hydrogen peroxide) and transfer to solution oxidants (Ox), such as oxygen

$$e(TiO_2) + h_s^+ \xrightarrow{k_r} ... \quad (4)$$

where k_r and k_{ct} are the kinetic constants for electron recombination and transfer to solution, respectively. Both processes should be first order in electron concentration.

$$e(TiO_2) + Ox \xrightarrow{k_{ct}} ... \quad (5)$$

However, most photogenerated electrons are probably trapped electrons, which are supposed to play a crucial role in electron recombination and transfer to solution. According to Bisquert and Vikhrenko,[38] we may assume a quasiequilibrium condition for electrons, meaning that free and trapped electrons maintain a common equilibrium even when the system is displaced away from equilibrium. However, the determination of the total number of photogenerated electrons on the basis of open circuit photopotential measurements would require a knowledge of the density of electron trap states.

We are interested in evaluating the rate of electron decay as a function of the total concentration of photogenerated electrons in a nanocrystalline oxide thin film because of its relevance in heterogeneous photocatalysis. This can be achieved through a combination of photopotential decay measurements together with voltammetric experiments. In fact, the voltammetric behavior of nanoporous, nanoparticulate semiconductor oxide thin films is characterized by the appearance of capacitive currents due to the accumulation of electrons in the film, whose charge is screened by adsorbed/inserted protons (cations). Importantly, for weak electron accumulation, and if recorded at relatively low sweep rates, the voltammograms are virtually reversible.[39] Therefore, integration of the voltammogram results in accumulated charge, or equivalently electron density, as a function of the applied potential.

In the following, we illustrate such a procedure on the basis of experimental results obtained for a TiO_2 electrode in contact with a 0.1 M $HClO_4$ solution (Figure 1; see caption for experimental details). The experimental results needed to perform the intended kinetic analysis are (1) a cyclic voltammogram (I vs E curve) recorded in the dark at a relatively low sweep rate (υ), leading to a quasireversible profile (Figure 1A) and (2) the E_{oc} vs t relaxation curve obtained upon interrupting continuous stationary illumination (Figure 1B). At each time t during the relaxation, the value of E_{oc} can be read and the corresponding concentration of photogenerated electrons (n_{ph}) calculated as

$$n_{ph} = \frac{1}{eAd} \int_{E_{oc}^{dark}}^{E_{oc}(t)} \frac{I}{\upsilon} dE \quad (6)$$

where A is the geometric area of the thin film and d is its thickness (Figure 1C). Once $n_{ph}(t)$ is known the corresponding first-order reaction constants as a function of the electron concentration, $\bar{k}$, can be obtained (Figure 1D) as

$$\bar{k} = -\frac{1}{n_{ph}} \frac{dn_{ph}}{dt} \quad (7)$$

If the experiments are done in the absence of an effective oxidant, the first-order rate constant will correspond mainly to recombination processes (reaction 4), whereas in the presence of an oxidant such as oxygen, the constant will correspond to the transfer of electrons from the nanoparticulate sample to the oxidant present in solution (reaction 5). The calculation of a first-order rate constant is merely formal in the case of the recombination process because the concentration of trapped holes is not a controllable independent variable but rather is closely related to the stationary concentration of electrons achieved by illumination.

The values obtained as illustrated in Figure 1 correspond to the average rate constants for all of the photogenerated electrons

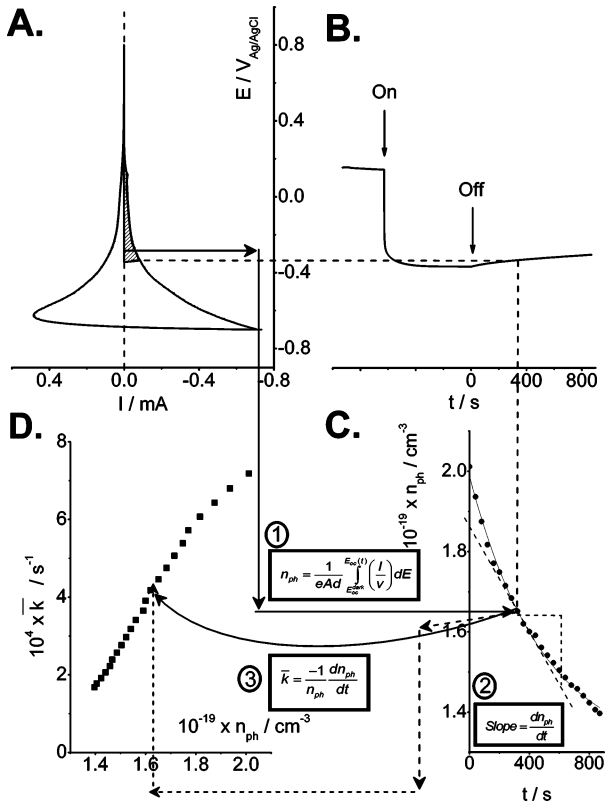

Figure 1. Illustration of the pseudo-first-order rate constant calculation algorithm. The electrode was a P25 nanocrystalline thin film in contact with a N_2-purged 0.1 M $HClO_4$ solution (electrode thickness, 7 μm; electrode exposed area, 1.54 cm^2; incident light intensity, 0.24 W) (A) Cyclic voltammogram obtained in the dark (10 mV/s), (B) (Photo)-potential transient decay obtained after the electrode was illuminated, (C) Photogenerated electron concentration variation with time, obtained from (A) and (B) data, and eq 1. (D) Pseudo-first-order rate constant variation with photogenerated electron concentration, obtained from (C) data and eqs 2 and 3.

contained in the film. Likewise, $\bar{k}(n_{ph})$ can be converted into $\bar{k}(E)$. Again the value thus obtained would correspond to the average value of the recombination constant for the electrons having a potential higher than E.

In this context it will be particularly interesting to obtain values for $k(E)$, i.e., the value of the rate constant for defined values of the electron potential energy. We may describe such constants as microcanonical. Scheme 1 shows in a graphic way the different processes to which the rate constants are associated both in the presence and in the absence of oxidants in solution. There are two constants denoted by the subscript r, corresponding to the recombination of electrons with surface trapped holes and two other corresponding to the reduction of a deliberately added oxidant (O_2) and labeled with the subscript ct. As depicted in the scheme, the recombination process occurs in an inelastic way, through empty surface states (trapped holes), whereas electron transfer to solution occurs in an isoenergetic way, particularly when the oxidant does not interact strongly with the oxide surface. It is worth noting that there will be a direct correlation between electron potential energy and electrode potential as long as there is no change in the potential drop of the Helmholtz layer ($\Delta\phi_H$). However, in the course of the experiment described above, there is a net electron accumulation in the film upon illumination that could lead to a change in the potential drop through the Helmholtz layer. This fact should be kept in mind when interpreting the experimental results.

SCHEME 1: Energy Diagram Illustrating the Different Interfacial Processes Involved in the Photogenerated Electron Decay in the Dark[a]

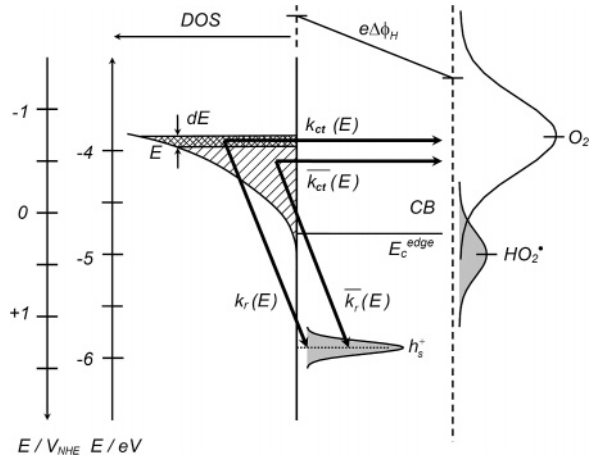

[a] $\bar{k}_{ct}(E)$ and $\bar{k}_r(E)$ are, respectively, the average rate constant for electron transfer to an oxidant in solution (O_2 in this case) and for electron recombination with surface trapped holes (h_s^+), $k_{ct}(E)$ and $k_r(E)$ are the microcanonical rate constants for electrons transferring to an oxidant and recombining with surface trapped holes, respectively. $\Delta\phi_H$ stands for the Helmholtz layer potential drop. The diagram energy levels approximately refer to a P25 nanocrystalline electrode in contact with a solution of pH 3.5.

Let us see how we can work out the $k(E)$ values. Taking into account that

$$\frac{dn_{E_{oc}^{dark},\,E+dE}}{dt} = \frac{dn_{E_{oc}^{dark},\,E}}{dt} + \frac{dn_{E,E+dE}}{dt} \tag{8}$$

where the subindices refer to a determined range of potentials, and according to the definitions of first-order rate constants

$$-\frac{dn_{E,E+dE}}{dt} = k(E)n_{E,E+dE} = \bar{k}(E+dE)n_{E_{oc}^{dark},\,E+dE} - \bar{k}(E)n_{E_{oc}^{dark},\,E} \tag{9}$$

Substituting the expressions $\bar{k}(E + dE)$ and $n_{E_{oc}^{dark},\,E+dE}$ with their series expansions truncated at the first term

$$\bar{k}(E+dE) = \bar{k}(E) + \left(\frac{d\bar{k}(E)}{dE}\right)dE \tag{10}$$

and

$$n_{E_{oc}^{dark},\,E+dE} = n_{E_{oc}^{dark},\,E} + n_{E,E+dE} = n_{E_{oc}^{dark},\,E} + \left(\frac{dn_{E_{oc}^{dark},\,E}}{dE}\right)dE \tag{11}$$

By substituting eqs 10 and 11 into eq 9 and neglecting the second order differentials, the following equation results:

$$k(E)\frac{dn_{E_{oc}^{dark},\,E}}{dE} = n_{E_{oc}^{dark},\,E}\frac{d\bar{k}(E)}{dE} + \bar{k}(E)\frac{dn_{E_{oc}^{dark},\,E}}{dE} \tag{12}$$

which can be rewritten as

$$k(E) = \bar{k}(E) + n_{E_{oc}^{dark},\,E}\left(\frac{d\bar{k}(E)}{dE}\right)\left(\frac{dE}{dn_{E_{oc}^{dark},\,E}}\right) \tag{13}$$

The value of $dE/dn_{E_{oc}^{dark},\,E}$ can be obtained directly from cyclic voltammetry, which finally leads to

$$k(E) = \bar{k}(E) + n_{E_{oc}^{dark},\,E}\, eAd\, \frac{\upsilon}{I(E)} \left(\frac{d\bar{k}(E)}{dE}\right) \qquad (14)$$

Alternatively, from eq 13, we may write down

$$k(E) = \bar{k}(E) + n_{E_{oc}^{dark},\,E} \left(\frac{d\bar{k}}{dn_{E_{oc}^{dark},\,E}}\right) \qquad (15)$$

which allows for a determination of the second right-hand term from $\bar{k}(n_{ph})$ plots.

In principle, the first-order rate constant is expected to vary as the average energy of the electrons contained in the film changes. This average is related to the fraction of electrons that are trapped as well as to the depth of the traps.

Experimental Section

Chemicals. All chemicals were used as received without further purification. Working solutions were prepared with ultrapure water (Millipore MilliQ). Sodium perchlorate monohydrate (extra pure) was supplied by Scharlau. Perchloric acid (p.a., 60%), sodium hydroxide (p.a.), and hydrofluoric acid (p.a., 48%) were supplied by Merck. Solution pH was adjusted to 3.5 using either 1 M NaOH or 1 M $HClO_4$. Titanium dioxide nanoparticles were obtained from Alfa Aesar (anatase, 32 nm, 99.9%), PI-KEM Ltd. (rutile-rich, 35 nm, 99%), and Degussa-Hüls (P25, 20 nm). These samples were characterized in ref 39. The oxide slurry for deposition was made using Triton X-100 and acetylaceton 99% from Aldrich.

Preparation of Nanocrystalline Thin Films. The semiconductor oxide slurry was prepared as follows. A total of 330 μL of MilliQ distilled water was mixed with 30 μL of acetylacetone in a mortar; 1 g of the commercial nanoscopic powder was added and ground with the solution for 15 min until a homogeneous slurry was obtained. Then, 1.3 mL of distilled water were added dropwise. A dispersion with a 60 wt % of the oxide was formed, and 20 μL of the tensioactive Triton X-100 were added to stabilize the dispersion. Then, 15−20 μL of the suspension were spread over around 2 cm^2 of a FTO substrate (U-type Asahi Glass Co., Japan) using the doctor-blade method. Finally, the nanocrystalline thin film was thermally annealed in air for 1 h at 450 °C. The resulting film average thickness was 2 μm for anatase, 10 μm for P25 and 11 μm for PI-KEM.

Apparatus. The electrochemical measurements were performed using a standard photoelectrochemical setup. It was composed of a computer-controlled potentiostat, μAUTOLAB type III, and a 150 W Bausch&Lomb Xe arc lamp as illumination source. The electrochemical cell was a conventional three-electrode cell with a 1 mm thick fused silica window. The counter and reference electrodes were a Pt wire and a Ag/AgCl/KCl(sat) electrode, respectively. The working solutions were 0.5 M $NaClO_4$ with or without 0.01 M (HF + NaF), buffered to pH 3.5 purged with nitrogen (or oxygen). Incident light intensity was measured with an optical power meter (Oriel model 70310) equipped with a thermopile head (Ophir Optronics 71964). The electrode thickness was determined by SEM measurements, using a HITACHI S-3000N microscope.

Results and Discussion

Absence of Dissolved Oxygen. The illumination of a TiO_2 film yields free electrons and holes. Whereas the holes get quickly trapped, eventually giving rise to different oxidized adsorbed species, a substantial amount of the photogenerated electrons remain as free carriers in the conduction band, although they can also get trapped. As mentioned above, a quasiequilibrium likely exists between trapped and free electrons, even when the system is out of equilibrium.[38] In any case, the decay in photopotential and, thus, in electron concentration once the illumination is interrupted is mainly due to reaction 4. In this respect, it is worth noting that photogenerated trapped holes have a long lifetime in the absence of solution hole acceptors. In fact, already in 1980, Wilson demonstrated by means of voltammetric experiments that the surface states produced by hole oxidation were stable for minutes.[40] Later Nakato and co-workers reproduced such behavior[41,42] and finally assigned these oxidized surface states to surface trapped holes.[43] Figures 2−4 show the cyclic voltammograms and the photopotential transients recorded for anatase (Alfa-Aesar), P25, and PI-KEM electrodes, respectively, both in the absence and in the presence of fluoride. As observed, the photopotential relaxation follows different kinetics depending on the nature of the particular TiO_2 sample employed to prepare the electrodes. This means that the kinetics of the electron/trapped hole recombination depends, as expected, on the (surface) structure of the sample under study. The relaxation times attain values of the order of minutes. This is not unexpected on the basis of the high stability of the trapped holes mentioned above.[40]

A quantitative analysis has been done according to the procedure delineated in the Theory section, which entails the obtainment of values for the apparent first-order kinetic constants of electron recombination. The computed kinetic constant values are presented in Figure 5. As expected, these depend on the value of the total electron density in the nanocrystalline film, i.e., on the value of the potential energy for the electrons. As the electron density grows, an increasing fraction of the photogenerated electrons is expected to correspond to free CB carriers. In any case, the photogenerated electrons are energetically located close to the CB edge, in the region of the exponential distribution proposed for nanocrystalline electrodes.[23,44] These states have been spatially located at the TiO_2 surface. One would expect that the higher the electron concentration (and average potential energy), the higher the recombination constant. This is the case for anatase and, partly, for P25 samples. In addition, for both PI-KEM and P25 thin films, there is an increase in the rate constant for low electron densities. The reason could be that electrons in shallow traps at the surface are more reactive with trapped holes because of spatial proximity. This will depend obviously on the particular surface structure of the sample and on the location of the hole and electron surface traps. The case of P25 is particularly interesting because of a nonmonotonic behavior, suggesting a separate reactivity of free and trapped electrons.

A more accurate analysis can be done if the corresponding microcanonical constants $k(E)$ are calculated. As observed in Figure 6, similar tendencies are observed. Significantly, higher electron reactivity is found for electrons at potentials less negative than −0.2 V, whose voltammetric signal (shoulder in the dn/dE vs E curve of Figure 6) lies at the very onset of the accumulation region. Recently, we have seen evidence that they are actually trapped at GBs.[39,45] The results shown here indicate that they would behave efficiently as recombination centers, thus increasing the electron consumption constant. This means that surface trapped holes should be able to diffuse to the particle GBs. In fact, Nakato and co-workers attributed a high mobility to surface trapped holes when proposing a mechanism for the photoinduced oxygen evolution.[43] When the remaining concentration of carriers (electrons and holes) is low enough and most of the remaining electrons are trapped at GBs, surface trapped

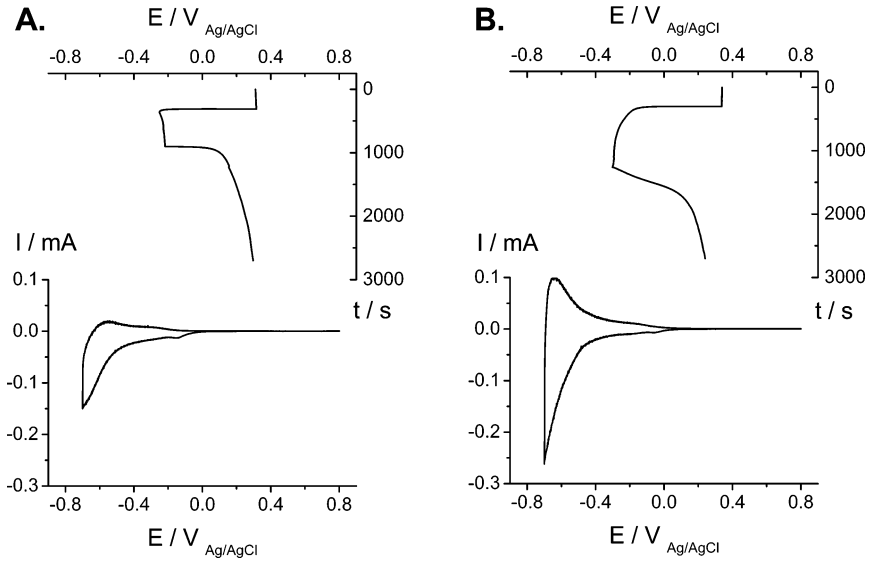

Figure 2. Cyclic voltammogram (10 mV/s) and (photo)potential transient decay curves for an anatase nanocrystalline thin film in contact with a N_2-purged solution of (A) 0.5 M $NaClO_4$ and (B) 0.5 M $NaClO_4$, 0.01 M (HF + NaF). Electrode thickness, 2 μm; electrode exposed area, 2.00 cm^2; incident light intensity, 0.36 W. All solutions were buffered at pH 3.5.

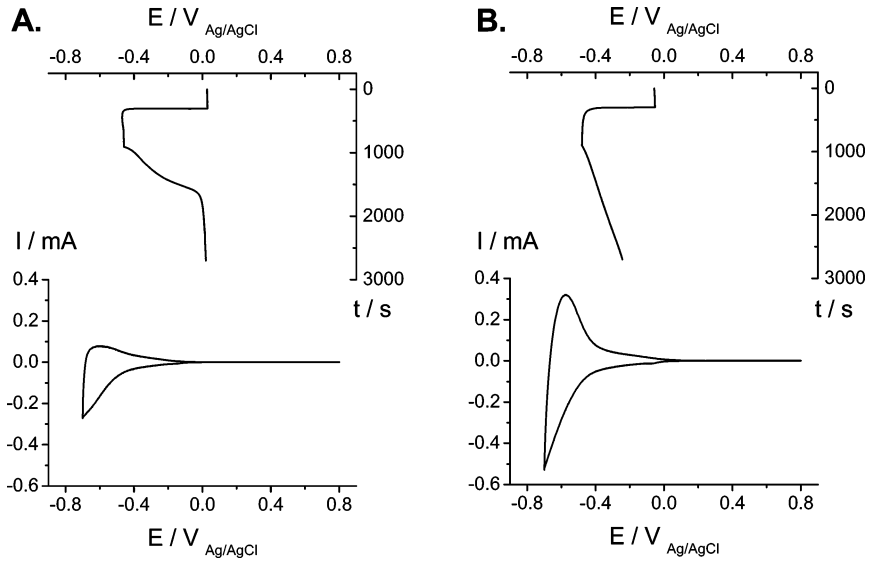

Figure 3. Cyclic voltammogram (10 mV/s) and (photo)potential transient decay curves for a P25 nanocrystalline thin film in contact with a N_2-purged solution of (A) 0.5 M $NaClO_4$ and (B) 0.5 M $NaClO_4$, 0.01 M (HF + NaF). Electrode thickness, 10 μm; electrode exposed area, 1.68 cm^2; incident light intensity, 0.27 W. All solutions were buffered at pH 3.5.

holes would be electrostatically attracted toward the GBs because these charges would not be screened by ions in solution. This would increase the recombination effective cross section, giving rise to the observed increase in the rate constant. Similar models have been proposed to explain the electrical properties of polycrystalline silicon films.[46] On the other hand, the tendency observed for electrons with higher energies (potential below −0.35 V) would correspond to either free or shallowly trapped electrons. An increased mobility could favor their higher reactivity with surface trapped holes. Interestingly, electrons of intermediate energy show very little reactivity toward recombination (constants around 2 orders of magnitude lower than in previous cases). This is reflected in the shoulder appearing in the potential relaxation curve, which was already clearly observed in the pioneering work by Kamat and co-workers.[7]

Adding fluoride to the system brings about a change in the dark open circuit potential, which tends to be lower (by up to 0.2 V) as corresponds to an anionic adsorption that shifts the bands downward in the electrode potential scale (upward in the electron potential energy scale). In addition, there is a drastic change in the voltammetric profile in the accumulation region (increase of electrode capacitance). More importantly, and as observed in Figures 2−4, there is a significant retardation of the photopotential relaxation. In Figure 5, the corresponding values of the first-order rate constants are given. As observed, the introduction of fluoride has two main effects: (i) the first-order electron recombination constant drops by 1−2 orders of magnitude and (ii) it becomes virtually independent of the electron concentration. Both effects can be rationalized on the basis of previous explanations on the behavior of fluorinated TiO_2 surfaces.

Fluoride has been proposed to hinder hole trapping, favoring the formation of free solution hydroxyl radicals. This would lead to a drastic diminution in the electron recombination rate as observed in the experiments. Alternatively, we believe that the introduction of fluoride would lead not only to an upward shift of the TiO_2 bands but also to an upward shift of the electronic traps relative to the bands because of the preferential

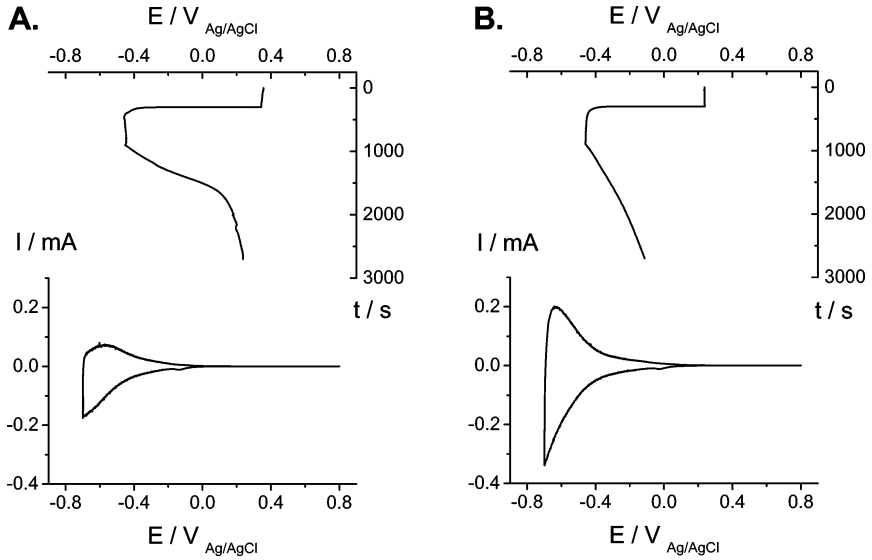

Figure 4. Cyclic voltammogram (10 mV/s) and (photo)potential transient decay curves for a PI-KEM nanocrystalline thin film in contact with a N_2-purged solution of (A) 0.5 M $NaClO_4$ and (B) 0.5 M $NaClO_4$, 0.01 M (HF + NaF). Electrode thickness, 11 μm; electrode exposed area, 1.61 cm^2; incident light intensity, 0.26 W. All solutions were buffered at pH 3.5.

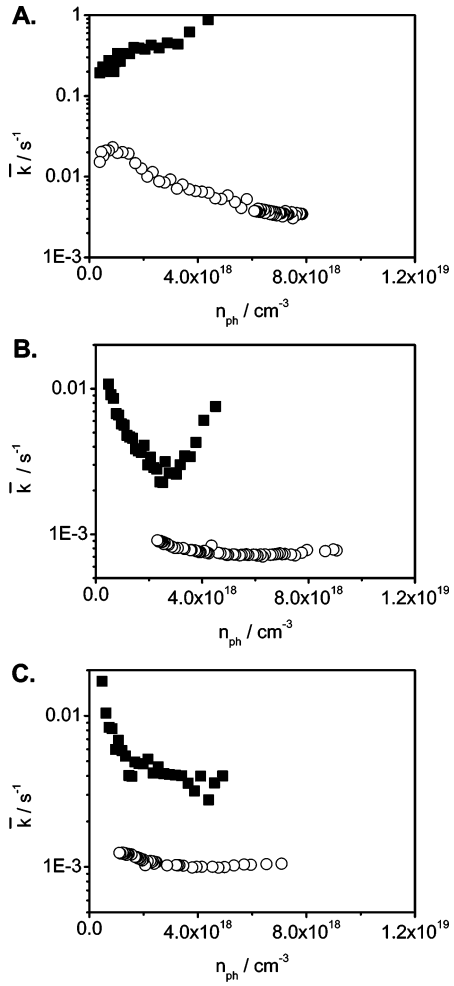

Figure 5. Average of the pseudo-first-order rate constants calculated according to eqs 6 and 7, for an (A) anatase, (B) P25, and (C) PI-KEM nanocrystalline thin film in contact with a N_2-purged solution of 0.5 M $NaClO_4$ (black squares) or 0.5 M $NaClO_4$ and 0.01 M (HF + NaF) (open circles). Other experimental conditions as in Figures 2−4.

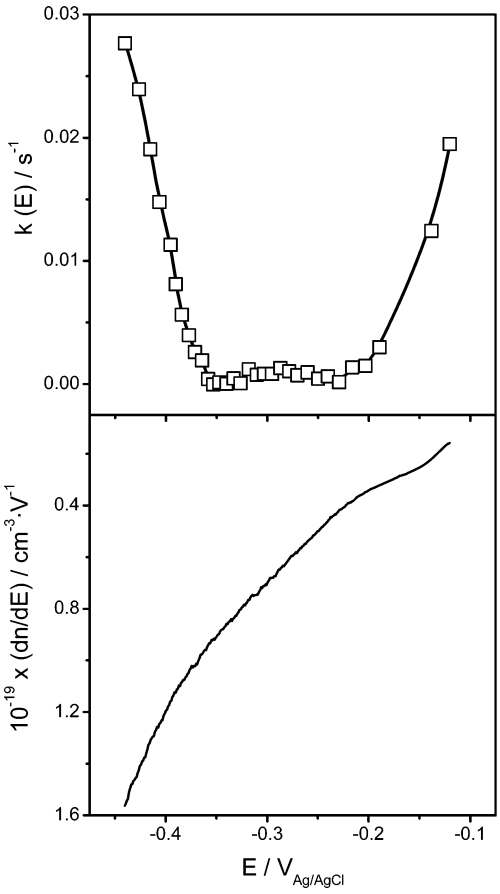

Figure 6. Microcanonical first-order rate constants calculated for a P25 nanocrystalline thin film in contact with a N_2-purged 0.5 M $NaClO_4$ solution (pH 3.5). Other conditions as in Figure 5.

complexation of fluoride to Ti(IV) rather than to Ti(III). In such a way, both the concentration of trapped electrons and the rate of recombination between trapped electrons and holes would diminish. However, in the literature, other explanations for the reduction in electron reactivity can be found. According to Choi and co-workers,[30] the photogenerated electrons are thought to be less reactive because of the effectiveness of the ≡Ti−F sites as traps. The strong electronegativity of fluorine would lead to a tight holding of trapped electrons, which would become less labile. Significantly, Calza et al.[47] have suggested that the

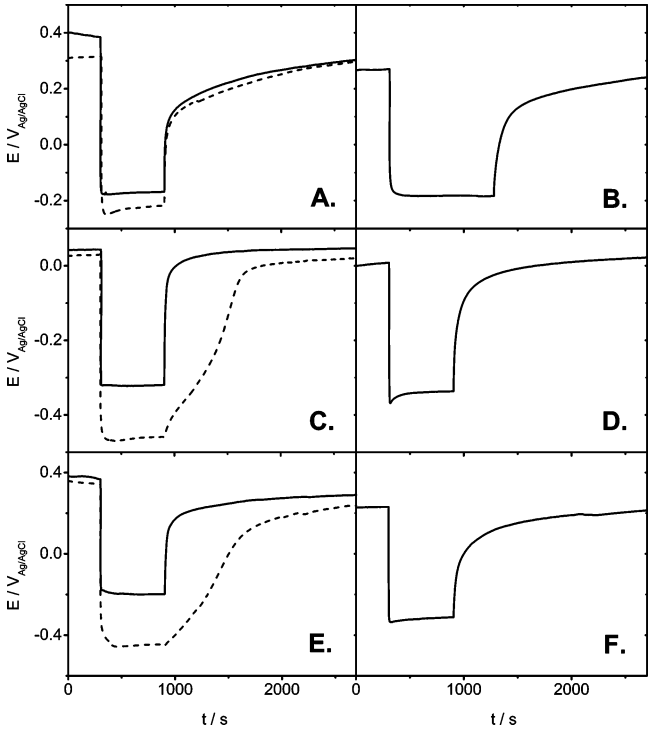

Figure 7. (Photo)potential decay transients for O_2-purged 0.5 M $NaClO_4$ solutions, in the presence (B, D, F) and in the absence of 0.01 M (HF + NaF) (A, C, E), using an anatase (A, B), a P25 (C, D), or a PI-KEM (E, F) nanocrystalline electrode. N_2-purged transients are shown with dashed line for comparison. All solutions were buffered at pH 3.5. Other experimental conditions as in Figures 3−5.

probability of recombination of the photogenerated electron−hole pairs is also lowered upon fluorination.

Let us discuss the fact that the kinetic recombination constant becomes barely dependent on electron concentration upon fluorination. As commented above, we believe that many surface electron traps are lost as they become energetically located inside the conduction band. Such a reduction in the number of traps should lead to a predominance of trapped hole recombination with free electrons over recombination between trapped carriers. One would expect more homogeneous reactivity for free electrons than for surface trapped electrons, for which locations significantly different, both sterically and energetically, are possible. Alternatively, electron recombination with solution radicals would also lead to reaction constants less dependent on electron concentration (or potential) because the complexities derived from different locations for surface trapped holes would disappear.

Presence of Dissolved Oxygen. As observed directly from the photopotential experiments (Figure 7), in the presence of oxygen there is a drastic acceleration of the potential relaxation process (except for anatase). This is a result of the predominance of reaction 5 in the consumption of photogenerated electrons.

Figure 8 shows the plots of the first-order kinetic constants for the consumption of electrons. Concretely, there is an increase of more than 1 order of magnitude in the value of the electron consumption constant upon the introduction of oxygen. Interestingly, except for anatase, the constant does not depend in an important way on the electron potential energy, suggesting that the species being reduced is adsorbed oxygen, which could capture free electrons in an inelastic way.

The adsorption of fluoride triggers important changes in the behavior of the system. On the one hand, there is a significant decrease in the first-order kinetic constant and, on the other,

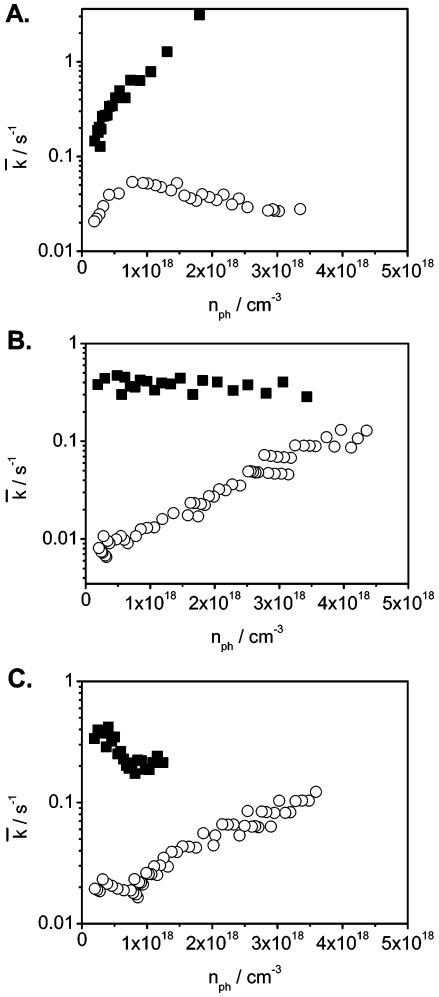

Figure 8. Average of the pseudo-first-order rate constants calculated according to eqs 6 and 7, for an (A) anatase, (B) P25, and (C) PI-KEM nanocrystalline thin film in contact with an O_2-purged solution of 0.5 M $NaClO_4$ (black squares) or 0.5 M $NaClO_4$ and 0.01 M (HF + NaF) (open circles). All solutions were buffered at pH 3.5. Other experimental conditions as in Figures 3−5.

except for anatase, the values of the constant become dependent on the electron concentration (and, thus, on the electron energy): The higher the electron energy, the higher the value for the kinetic constant. This is understandable on the basis of the complexation by fluoride of the Ti(IV) sites. In fact, it has been observed that the adsorption of different species such as formic acid, catechol, and H_2O_2 is impaired by fluorination.[25,36] The same behavior is expected in the case of O_2, which is not thought to be strongly adsorbed. Once displaced from the surface, the reduction of oxygen should involve dissolved oxygen molecules, on the one hand, and CB electrons, on the other. As mentioned above, the adsorption of fluoride is expected to significantly diminish the number and depth of electron traps. In such a case, and taking into account the electrode potential of the O_2/HO_2 couple, the observed behavior is understandable on the basis of the Gerischer's theoretical expression for an outer sphere, isoenergetic, electron-transfer process[5,48]

$$k(E) = k(E)_{\max} \exp\left[-\frac{(E(e_{ph}^-) - E^o_{O_2})^2}{4kT\lambda}\right] \qquad (16)$$

where $E^o_{O_2}$ represents the value of the most probable energy level for the oxidant (O_2 in our case), $E(e_{ph}^-)$ represents the potential energy for TiO_2 CB electrons and λ denotes the

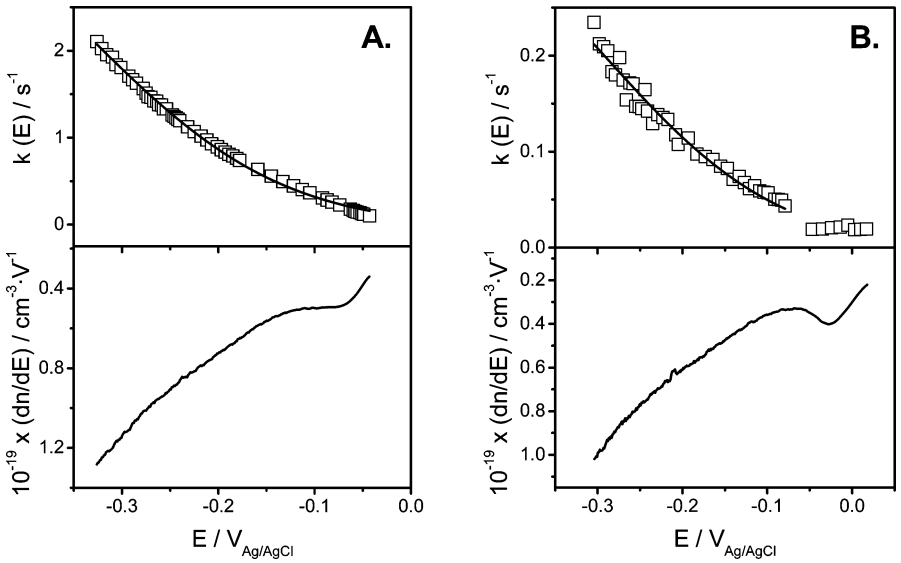

Figure 9. Microcanonical first-order rate constants calculated for a (A) P25, (B) PI-KEM nanocrystalline thin film in contact with an O_2-purged 0.5 M $NaClO_4$, 0.01 M (HF + NaF) solution (pH 3.5). Other conditions as in Figure 7. Solid lines: fit to the Gerischer model (eq 16).

reorganization energy for the O_2/HO_2 redox couple. The approximate situation shown in Scheme 1 corresponds to a pH value of 3.5. As deduced from eq 16 (or from Scheme 1), within the energy range attainable for the photogenerated electrons, the higher the electron potential energy, the larger the corresponding density of empty states of the redox system and, consequently, the higher the value of the charge-transfer constant. Remarkably, this is the behavior observed clearly for both PI-KEM and P25 electrodes. Figure 9 shows the values of the microcanonical first-order decay constants for the latter cases. In the case of the PIKEM sample (Figure 9B), two regions can be distinguished: for electrons at the onset of the accumulation region the charge-transfer constants are relatively low and virtually independent of the electrode potential, whereas for more negative potential values, a kinetic constant growing approximately in an exponential way is found. A simpler behavior is found in the case of the P25 thin film: a microcanonical constant growing exponentially as the potential is made more negative is found. Interestingly, the experimental constant can be fitted reasonably to eq 16 as demonstrated by the solid lines in Figure 9. The values found for k_{ox}^{max} were 3.4 and 0.42 s^{-1} for P25 and PIKEM respectively, whereas the value of $E^{o}_{O_2}$ employed in both cases corresponds to a potential of -0.52 $V_{Ag/AgCl}$ (-0.32 V_{NHE}). This value is reasonable on account of the tabulated standard potential value for the O_2/HO_2 redox couple (-0.05 V_{NHE}), the possibility of HO_2 adsorption and the uncertainties in the interfacial pH value in the solution within the porous oxide matrix. Finally, the value for the reorganization energy used in both cases was of 0.72 eV.

Conclusions

An electrochemical method has been presented for the obtainment of electron concentration decay curves for nanocrystalline TiO_2 thin films after light interruption once a photostationary state was attained. The method entails measuring the open circuit potential relaxation curves together with cyclic voltammograms for the nanocrystalline thin films in the electron accumulation region. From the integration of the voltammogram, the electron concentration is obtained as a function of the electrode potential, and therefore, the E_{oc} vs t relaxation curve can be converted into an electron concentration versus time curve. The latter can be the basis for the calculation of (pseudo) first-order electron consumption constants. In addition of average constants (for all the photogenerated electrons present in the film), a method is proposed for the obtainment of microcanonical constants, that is, of constants depending on the energy (redox potential) of the electrons in the film.

Such simple measurements are potentially of high interest in aqueous solution heterogeneous photocatalysis. They can furnish values of kinetic constants for either the recombination process (with trapped holes) or the reduction of oxygen molecules depending on the solution composition. If the solution is purged with nitrogen, the electrons are consumed mainly through their recombination with surface trapped holes, whereas charge transfer to solution O_2 is mainly responsible for the electron decay when the experiments are done in oxygen-purged solutions.

We have applied these measurements to both electron recombination and charge-transfer processes for different TiO_2 nanoparticulate thin films before and after fluorination, which is known to cause an important effect on their photocatalytic behavior. The main results gathered prior to fluorination are as follows: (i) the kinetic constants depend strongly on the particular sample being employed. This is expected because the processes being analyzed occur at the oxide/solution interface, which is expected to vary strongly from sample to sample. (ii) In the case of P25 (and PIKEM) thin films, there is a distinct behavior for the electrons associated to the band gap traps appearing in the voltammetric experiment at the beginning of the accumulation region, being characterized by an enhanced recombination constant. In fact, this can already be gleaned from the shape of the potential relaxation curve, which shows a clear-cut shoulder. This agrees with our ascription of these states to traps at the grain boundaries.[39,45] It appears then that such electron traps would act as recombination centers. For practical purposes, their concentration should be minimized.

Upon the addition of fluoride, the behavior of the different samples both in the presence and in the absence of oxygen is more homogeneous. Both recombination and charge transfer to solution get retarded, especially the former. Interestingly, for both PIKEM and P25 thin films, the kinetic constant for charge transfer to solution depends on the electrode potential according to the Gerischer model (eq 16), employing the same values for

the O_2/HO_2 redox couple equilibrium potential and the reorganization energy. The experiments presented here allow us to both confirm in a direct way and quantify some hypotheses formulated on the basis of photocatalytic and photoelectrochemical experiments. In this way, on several occasions, it has been suggested that, upon fluorination, there is a reduction of the interfacial electron-transfer rates.[30,37] The results obtained in the presence of oxygen and the subsequent discussion provide compelling evidence on the retardation of the interfacial charge transfer to oxygen. A decreased rate of recombination as proposed by Calza et al.[47] is directly understandable on the basis of the experiments done in the absence of a dissolved oxidant.

Acknowledgment. Financial support from the Spanish Ministry of Education and Science (MEC) through Projects HOPE CSD2007-00007 (Consolider-Ingenio 2010) and CTQ2006-06286 (Fondos FEDER) as well as from the Generalitat Valenciana (ACOMP07-095) is gratefully acknowledged. D.M.-S. is grateful to MEC for the award of a FPI grant.

References and Notes

(1) O'Regan, B.; Grätzel, M. *Nature (London)* **1991**, *353*, 737.
(2) Takabayashi, S.; Nakamura, R.; Nakato, Y. *J. Photochem. Photobiol. A* **2004**, *166*, 107.
(3) Uzunova, M.; Kostadinov, M.; Georgieva, J.; Dushkin, C.; Todorovsky, D.; Philippidis, N.; Poulios, I.; Sotiropoulos, S. *Appl. Catal. B* **2007**, *73*, 23.
(4) Hoffmann, M. R.; Martin, S. T.; Choi, W.; Bahnemann, D. W. *Chem. Rev.* **1995**, *95*, 69.
(5) Nozik, A. J.; Memming, R. *J. Phys. Chem.* **1996**, *100*, 13061.
(6) Serpone, N.; Emeline, V. *Res. Chem. Intermed.* **2005**, *31*, 391.
(7) Vinodgopal, K.; Hotchandani, S.; Kamat, P. V. *J. Phys. Chem.* **1993**, *97*, 9040.
(8) Zaban, A.; Greenshtein, M.; Bisquert, J. *Chem. Phys. Chem.* **2003**, *4*, 859.
(9) Bisquert, J.; Zaban, A.; Greenshtein, M.; Mora-Seró, I. *J. Am. Chem. Soc.* **2004**, *126*, 13550.
(10) Bailes, M.; Cameron, P. J.; Lobato, K.; Peter, L. M. *J. Phys. Chem. B* **2005**, *109*, 15429.
(11) Byrne, J. A.; Eggins, B. R. *J. Electroanal. Chem.* **1998**, *457*, 61.
(12) Byrne, J. A.; Davidson, A.; Dunlop, S. P. M.; Eggins, B. R. *J. Photochem. Photobiol. A* **2002**, *148*, 365.
(13) Sun, W.; Chenthamarakshan, C. R.; Rajeshwar, K. *J. Phys. Chem. B* **2002**, *106*, 11531.
(14) Tada, H.; Kokubu, A.; Iwasaki, M.; Ito, S. *Langmuir* **2004**, *20*, 4665.
(15) Lana-Villarreal, T.; Gómez, R. *Chem. Phys. Lett.* **2005**, *414*, 486.
(16) Lana-Villarreal, T.; Gómez, R. *Electrochem. Commun.* **2005**, *7*, 1289.
(17) Li, M. C.; Shen, J. N. *J. Solid State Electrochem.* **2006**, *10*, 980.
(18) Lyon, A.; L.; Hupp, J. T. *J. Phys. Chem. B* **1999**, *103*, 4623.
(19) Boschloo, G.; Fitzmaurice, D. *J. Phys. Chem. B* **1999**, *103*, 7860.
(20) Kavan, L.; Kratochvilová, K.; Grätzel, M. *J. Electroanal. Chem.* **1995**, *394*, 93.
(21) Boschloo, G.; Fitzmaurice, D. *J. Phys. Chem. B* **1999**, *103*, 2228.
(22) Wang, H.; He, J.; Boschloo, G.; Lindström, H.; Hagfeldt, A.; Lindquist, S.-E. *J. Phys. Chem. B* **2001**, *105*, 2529.
(23) Fabregat-Santiago, F.; Mora-Sero, I.; Garcia-Belmonte, G.; Bisquert, J. *J. Phys. Chem. B* **2003**, *107*, 758.
(24) Kormann, C.; Bahnemann, D. W.; Hoffmann, M. R. *Environ. Sci. Technol.* **1991**, *25*, 494.
(25) Minero, C.; Mariella, G.; Maurino, V.; Pelizzetti, E. *Langmuir* **2000**, *16*, 2631.
(26) Minero, C.; Mariella, G.; Maurino, V.; Vione, D.; Pelizzetti, E. *Langmuir* **2000**, *16*, 8964.
(27) Yu, J. C.; Yu, J.; Ho, W.; Jiang, Z.; Zhang, L. *Chem. Mater.* **2002**, *14*, 3808.
(28) Chiang, K.; Amal, R.; Tran, T. *J. Mol. Catal. A* **2003**, *193*, 285.
(29) Oh, Y.-C.; Jenks, W.S. *J. Photochem. Photobiol. A* **2004**, *162*, 323.
(30) Park, H.; Choi, W.; *J. Phys. Chem. B* **2004**, *108*, 4086.
(31) Watanabe, N.; Horikoshi, S.; Hidaka, H.; Serpone, N. *J. Photochem. Photobiol. A* **2005**, 174, 229.
(32) Lee, J.; Choi, W.; Yoon, J. *Environ. Sci. Technol.* **2005**, *39*, 6800.
(33) Park, H.; Choi, W. *Catal. Today* **2005**, *101*, 291.
(34) Kim, S.; Choi, W. *J. Phys. Chem. B* **2005**, *109*, 5143.
(35) Mrowetz, M.; Selli, E. *Phys. Chem. Chem. Phys.* **2005**, *7*, 1100.
(36) Maurino, V.; Minero, C.; Mariella, G.; Pelizzetti, E. *Chem. Commun.* **2005**, 2627.
(37) Mrowetz, M.; Selli, E. *New J. Chem.* **2006**, *30*, 108.
(38) Bisquert, J.; Vikhrenko, V. S. *J. Phys. Chem. B* **2004**, *108*, 2313.
(39) Berger, T.; Lana-Villarreal, T.; Monllor-Satoca, D.; Gómez, R. *Electrochem. Commun.* **2006**, *8*, 1713.
(40) Wilson, R. H. *J. Electrochem. Soc.* **1980**, *127*, 228−234.
(41) Nakato, Y.; Tsumura, A.; Tsubomura, H. *J. Phys. Chem.* **1983**, *87*, 2402−2405.
(42) Nakato, Y.; Akanuma, H.; Magari, S.; Yae, S.; Shimizu, J.-I.; Mori, H., *J. Phys. Chem. B* **1997**, *101*, 4934−4939.
(43) Nakamura, R.; Okamura, T.; Ohashi, N.; Imanishi, A.; Nakato, Y., *J. Am. Chem. Soc.* **2005**, *127*, 12975−12983.
(44) Abayev, I.; Zaban, A.; Kytin, V. G.; Danilin, A. A.; García-Belmonte, G.; Bisquert, J. *J. Solid State Electrochem.* **2007**, *11*, 647.
(45) Berger, T.; Lana-Villarreal, T.; Monllor-Satoca, D.; Gómez, R. *J. Phys. Chem. C.* **2007**, *111*, 9936.
(46) Seto, J. Y. W. *J. Appl. Phys.* **1976**, *46*, 5247.
(47) Calza, P.; Pelizzetti, E.; Mogyorósi, K.; Kun, R.; Dékány, I. *Appl. Catal. B* **2007**, 72, 314.
(48) Memming, R. *Semiconductor Electrochemistry*; Wiley-VCH; Weinheim, Germany, 2001.